Computing general geometric structures on surfaces using Ricci flow

Miao Jin[a], Feng Luo[b], Xianfeng David Gu[a,*]

[a] *Stony Brook University, United States*
[b] *Rutgers University, United States*

Abstract

Systematically generalizing planar geometric algorithms to manifold domains is of fundamental importance in computer aided design field. This paper proposes a novel theoretic framework, *geometric structure*, to conquer this problem. In order to discover the intrinsic geometric structures of general surfaces, we developed a theoretic rigorous and practical efficient method, *Discrete Variational Ricci flow*.

Different geometries study the invariants under the corresponding transformation groups. The same geometry can be defined on various manifolds, whereas the same manifold allows different geometries. Geometric structures allow different geometries to be defined on various manifolds, therefore algorithms based on the corresponding geometric invariants can be applied on the manifold domains directly.

Surfaces have natural geometric structures, such as spherical structure, affine structure, projective structure, hyperbolic structure and conformal structure. Therefore planar algorithms based on these geometries can be defined on surfaces straightforwardly.

Computing the general geometric structures on surfaces has been a long lasting open problem. We solve the problem by introducing a novel method based on discrete variational Ricci flow.

We thoroughly explain both theoretical and practical aspects of the computational methodology for geometric structures based on Ricci flow, and demonstrate several important applications of geometric structures: generalizing Voronoi diagram algorithms to surfaces via Euclidean structure, cross global parametrization between high genus surfaces via hyperbolic structure, generalizing planar splines to manifolds via affine structure. The experimental results show that our method is rigorous and efficient and the framework of geometric structures is general and powerful.
© 2007 Elsevier Ltd. All rights reserved.

Keywords: Geometric structure; Variational Ricci flow; Uniformization theorem; Hyperbolic structure; Projective structure; Spherical structure; Affine structure; Euclidean structure; Manifold spline

1. Introduction

Different geometries can be defined on the plane $\mathbb{R}^2$ and each of them studies different invariants under the corresponding transformation group of $\mathbb{R}^2$. The most common geometries on the plane are

(1) *Euclidean geometry*. The transformation group is the rigid motion group and each rigid motion has the form $\phi : \mathbb{R}^2 \to \mathbb{R}^2$

$$\phi(\mathbf{p}) = O\mathbf{p} + \mathbf{q}, \quad O \in SO(\mathbb{R}, 2), \mathbf{q} \in \mathbb{R}^2, \quad (1)$$

where O is a rotation matrix with determinant $+1$, and $SO(\mathbb{R}, 2)$ represents the 2 dimensional special real rotation

matrix group. The invariants are the *distance* between two arbitrary points, angles of corners, collinearity (i.e., all points lying on a line initially still lie on a line after transformation) etc.

(2) *Affine geometry*. The transformation group is the affine transformation group,

$$\phi(\mathbf{p}) = A\mathbf{p} + \mathbf{q}, \quad A \in GL(\mathbb{R}, 2), \mathbf{q} \in \mathbb{R}^2, \quad (2)$$

where A is a real matrix with a positive determinant, and $GL(\mathbb{R}, 2)$ denotes the 2 dimensional real general matrix group. The invariants are the collinearity, ratio between distances, and parallelism.

(3) *Projective geometry*. The transformation group is the real projective transformation, $\phi \in PGL(\mathbb{R}, 2)$ where $PGL(\mathbb{R}, 2)$ represents a 2 dimensional real projective matrix group,

$$\phi(x, y) = \left(\frac{\alpha x + \beta y + \gamma}{\delta x + \epsilon y + \zeta}, \frac{\eta x + \theta y + \kappa}{\delta x + \epsilon y + \zeta} \right),$$

* Corresponding author.
E-mail addresses: mjin@cs.sunysb.edu (M. Jin), fluo@math.rutgers.edu (F. Luo), gu@cs.sunysb.edu (X.D. Gu).
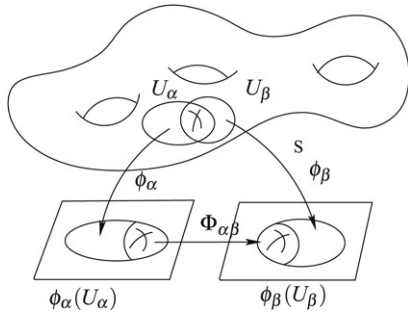
Fig. 1. Atlas: surface is covered by a set of charts (U_α, ϕ_α), where ϕ_α : $U_\alpha \to \mathbb{R}^2$. If two charts (U_α, ϕ_α) and (U_β, ϕ_β) overlap, the transition function $\phi_{\alpha\beta} : \mathbb{R}^2 \to \mathbb{R}^2$ is defined as $\phi_{\alpha\beta} = \phi_\beta \circ \phi_\alpha^{-1}$.

$$\begin{vmatrix} \alpha & \beta & \gamma \\ \eta & \theta & \kappa \\ \delta & \epsilon & \zeta \end{vmatrix} \neq 0. \tag{3}$$

The invariants are the colinearity and the cross ratio among four points on the line.

Different algorithms in computer graphics, computational geometry, solid modeling, and visualization are based on different geometries. The following are some examples:

(1) *Voronoi diagram.* Given a set of points $\{\mathbf{p}_k\} \subset \mathbb{R}^2$, the whole plane is partitioned to cells $\{C_k\}$. A point $\mathbf{p}$ belongs to C_k, where $k = \min_j |\mathbf{p} - \mathbf{p}_j|$. Therefore, the Voronoi diagram is based on planar Euclidean geometry, where distance plays vital role.

(2) *Point location.* Given a triangulation of the plane and an arbitrary point $\mathbf{p}$, the point location algorithm will find the unique triangle which contains $\mathbf{p}$. Suppose $\mathbf{p}$ is contained in a triangle $\Delta \mathbf{p}_0 \mathbf{p}_1 \mathbf{p}_2$, then every element of the barycentric coordinates of $\mathbf{p}(\alpha, \beta, \gamma)$ must be positive, where

$$\mathbf{p} = \alpha \mathbf{p}_0 + \beta \mathbf{p}_1 + \gamma \mathbf{p}_2.$$

It is obvious that barycentric coordinates are affine invariants. Therefore, the point location algorithm solely depends on the affine geometry of the plane.

(3) *Line segments intersection.* The sweep line algorithm computes all the intersections among a set of line segments on the plane. colinearity and intersection relations are invariant under projective transformation. Therefore, line segment intersection algorithms are based on the projective geometry of the plane.

One of the *fundamental problems* in graphics, geometric modeling, computational geometry and visualization is
To find feasible ways to define different geometries on surfaces, such that the algorithms designed for planar domains can be systematically and straightforwardly generalized to the surface domains.
Geometric structures offer theoretically rigorous and practically efficient solutions to this central problem.

1.1. Geometric structures

Suppose Σ is a surface in $\mathbb{R}^3$ as shown in Fig. 1. A family of open sets U_α covers the surface such that $\Sigma \subset \bigcup U_\alpha$. ϕ_α is

Table 1
Geometric structures on surfaces

(X, G) Structure	Parameter domain X	Trans. group, G	Oriented metric surfaces
Spherical	$\mathbb{S}^2$ Sphere	Rotation $SO(3)$	Genus zero closed, open
Euclidean	$\mathbb{R}^2$ Plane	Rigid motion	Genus one closed, open
Hyperbolic	$\mathbb{H}^2$ Hyperbolic space	Möbius	High genus closed, open
Affine	$\mathbb{R}^2$ Plane	Affine $GL(\mathbb{R}, 2)$	Genus one closed, open
Projective	$\mathbb{RP}^2$ Projective space	Projective	All oriented surfaces

a homeomorphism and maps U_α onto the plane:

$$\phi_\alpha : U_\alpha \to \mathbb{R}^2.$$

The pair (U_α, ϕ_α) is called a *local chart*. Suppose two open sets U_α and U_β intersect each other, then the *chart transition map* is defined as

$$\phi_{\alpha\beta} : \phi_\alpha(U_\alpha \cap U_\beta) \to \phi_\beta(U_\alpha \cap U_\beta), \quad \phi_{\alpha\beta} = \phi_\beta \circ \phi_\alpha^{-1}.$$

The union of all local charts $\{(U_\alpha, \phi_\alpha)\}$ form an *atlas*, denoted as $\mathscr{A}$. If all chart transition maps $\phi_{\alpha\beta}$ of $\mathscr{A}$ belong to the rigid motion group with the form in Eq. (1), then $\mathscr{A}$ is a *Euclidean atlas*. Similarly, if $\phi_{\alpha\beta}$ belongs to the affine transformation group with the form of Eq. (2) or projective transformation group with the form of Eq. (3), then $\mathscr{A}$ is called an *affine atlas* or *projective atlas*. Two Euclidean (affine or projective) atlases are *compatible*, if their union is still a Euclidean (affine or projective) atlas. A *Euclidean*, (*affine* or *projective*) *structure* of a surface Σ is the union of all its compatible Euclidean (affine or projective) atlases.

Euclidean, (*affine* or *projective*) *geometry* can be defined on the surface Σ via Euclidean (affine or projective) structure. Suppose surface Σ has a Euclidean atlas $\mathscr{A}$; we want to measure the distance between two points $\mathbf{p}$ and $\mathbf{q}$, which are close enough to be covered by a chart (U_α, ϕ_α). Then we measure the distance between $\phi_\alpha(\mathbf{p})$ and $\phi_\alpha(\mathbf{q})$ on the parameter domain $\phi_\alpha(U_\alpha)$. If $\mathbf{p}, \mathbf{q}$ are also covered by another chart (U_β, ϕ_β), we can similarly measure the distance between $\phi_\beta(\mathbf{p}), \phi_\beta(\mathbf{q})$ on the parameter domain $\phi_\beta(U_\beta)$. Because the transition map $\phi_{\alpha\beta}$ is a rigid motion on $\mathbb{R}^2$, it preserves distance. Therefore, the two measurements are consistent. In this way, we can define the distances between two arbitrary points on Σ, therefore Euclidean geometry is defined on Σ directly.

General (X, G) geometric structures can be defined in a similar way on a general surface Σ, where X is a topological space and G is the transformation group of X. An (X, G) *atlas* $\mathscr{A}$ of Σ is with chart transition maps $\phi_{\alpha\beta}$ in G and local parameters $\phi_\alpha(U_\alpha)$ in X. Two (X, G) atlases are *compatible*, if their union is still an (X, G) atlas. The union of all compatible (X, G)-atlases of Σ forms its (X, G) *structure*. The common (X, G) structures on surfaces are summarized in Table 1.

The existence of a specific geometric structure on a given surface is determined by the surface topology. Surfaces

with positive Euler numbers allow a spherical structure; surfaces with zero Euler numbers allow an affine [2,1] and Euclidean structure; surfaces with negative Euler numbers allow hyperbolic structure [4].

Conventional polar form splines are constructed from affine invariants, therefore, manifold splines are based on the affine structure of the surface. Because of topological obstruction, general surfaces do not admit affine structure. Projective structure exists for all oriented surfaces. If a spline scheme is based on projective invariants, it can be defined on all surfaces directly.

It is a very challenging problem to design a rigorous and practical methodology to compute general geometric structures on surfaces. Ricci flow is developed recently in geometric analysis field for the purpose of proving Poincaré conjecture. It offers a powerful tool to conquer this problem. To the best of our knowledge, we are the first group to design a discrete algorithm for computing hyperbolic structure and real projective structure on general surfaces, based on Ricci flow.

1.2. Ricci flow

Surface Ricci flow was first introduced by Hamilton in [11], and recently used to prove Poincaré conjecture [30–32]. Ricci flow was generalized to the combinational setting in [8]. The main idea is to conformally deform the Riemannian metric of the surface driven by its curvature, such that the curvature evolves like a heat diffusion and becomes a constant everywhere eventually. The metric with constant curvature is called uniformization metric. Ricci flow will deform the metric to the uniformization metric.

Suppose Σ is a surface with the metric tensor $g = (g_{ij})$, and K is the current Gaussian curvature, then Ricci flow is defined as

$$\frac{\partial g_{ij}}{\partial t} = -2K g_{ij}. \tag{4}$$

It is proven that the Ricci flow with normalized total surface area will flow the metric such that the Gaussian curvature on the surface is constant, namely the Gaussian curvature function $\lim_{t \to \infty} K(t, p)$ converges to a constant function.

In our paper, we use Ricci flow to compute uniformization metrics for surfaces with non-positive Euler numbers, from which we construct surface hyperbolic structure, real projective structure, and affine structure.

1.3. Contribution

This paper introduces a novel framework for geometric algorithm design: general geometric structures, such as affine structure, hyperbolic structure and real projective structure. Geometric structures allow different geometries to be defined on surfaces directly, and planar algorithms to be generalized to surfaces straightforwardly.

Compared to other structures, the hyperbolic structure and real projective structure have not been fully studied. This paper emphasizes on introducing novel and practical algorithms to compute hyperbolic structure and real projective structure

for general surfaces. The algorithm is based on a recently developed theoretical tool in the differential geometry field — Ricci flow. To the best of our knowledge, we are the first group to practically compute hyperbolic structure using Ricci flow, and also the first one to introduce a practical method to compute real projective structure. Therefore, the major contributions of this paper are:

- Introduce a novel theoretical framework: Geometric structures, which enable algorithms defined on planar domains to be systematically generalized to surfaces.
- Design and implement a novel geometric tool: discrete variational Ricci flow.
- Design and implement a practical and efficient algorithm based on Ricci flow to compute hyperbolic structures for surfaces with negative Euler number.
- Design and implement a practical and efficient algorithm based on Ricci flow to compute real projective structures for arbitrary surfaces.

2. Previous work

Geometric structures have been implicitly and explicitly applied in geometric modeling, computer graphics and medical imaging. For the genus zero case, the spherical structure was studied for texture mapping in [14,15] and for conformal brain mappings in [18,13]. Algorithms for computing conformal structures were introduced in [16,17], and the method is based on computing holomorphic differentials on surfaces.

Affine structure has been applied for constructing spline surfaces on general manifolds in [19], where the affine structures are induced by holomorphic differentials computed using the algorithms in [16,17].

Hyperbolic structure was applied in [9] for the topological design of surfaces, where the high genus surfaces were represented as quotient spaces of the Poincaré disk over Fuchsian group actions. In [5], Grimm and Hughes defined parameterizations for high genus surfaces and constructed functions on them. Wallner and Pottmann introduced the concept of spline orbifold in [7], which defined splines on three canonical parameter domains: the sphere, the plane, and the Poincaré disk. Hyperbolic geometry was visualized in [26]. The key difference between these works and our current one is that our method computes the hyperbolic metric which is conformal to the original metric on the surface, but their works only consider the topology and ignore the geometry of the surface. For many real applications, such as texture mapping, shape analysis and spline constructions, conformality between the original and the final metrics is highly desirable.

Recently, Goldman [29] examines some possible alternative mathematical foundations for computer graphics, such as Grassmann spaces and tensors. General geometric structures on manifolds contribute to the theoretical foundations for graphics and geometric modeling.

Ricci flow on surfaces was first introduced by Hamilton [11]. Ricci flow on 3-manifolds has been applied for the proof of Poincaré conjecture. Theoretical results of combinatorial Ricci flow have been summarized in [8]. Conventional Ricci flow can

(a) $\mathcal{X} > 0$.   (b) $\mathcal{X} = 0$.   (c) $\mathcal{X} < 0$.
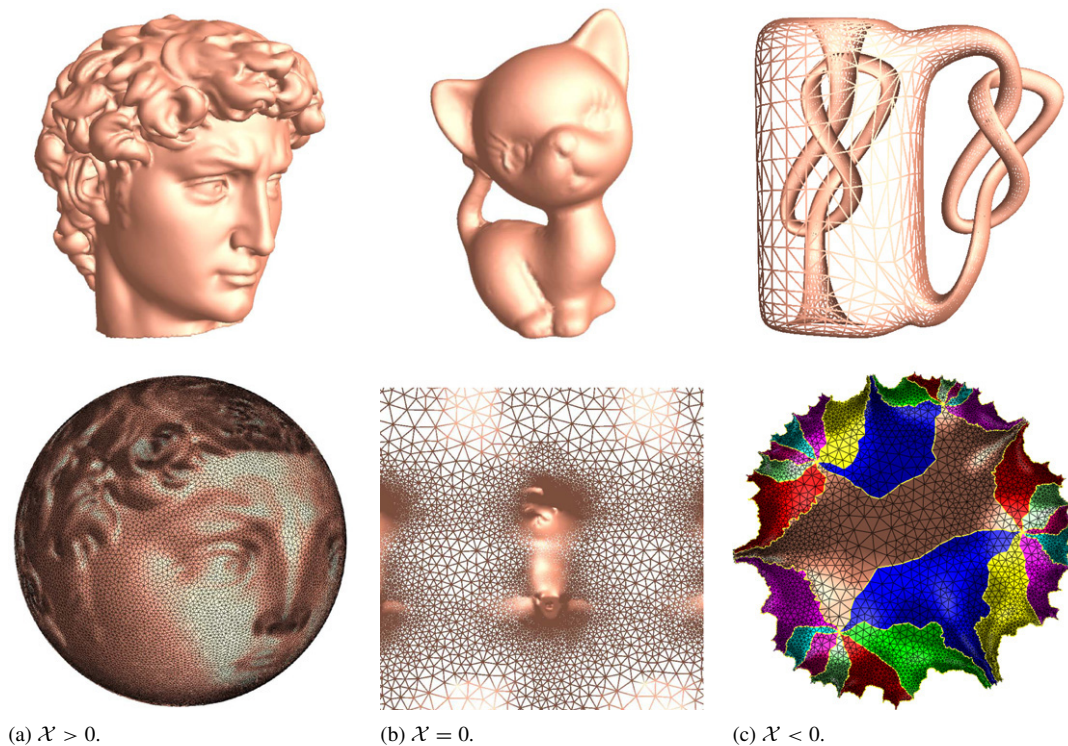
Fig. 2. Uniformization Theorem: all surfaces with Riemann metric can be conformally embedded into three canonical spaces: the unit sphere, the plane and the hyperbolic space. χ represents the Euler number of the surface.

be formulated as the gradient descent method for optimizing a special energy form, and the deficiency of its speed makes Ricci flow impractical. Practical algorithms are given in [25] for computing hyperbolic structures and real projective structures on surfaces. In our work, we improved the theoretical results in [8] by considering surface Riemannian metric induced from $\mathbb{R}^3$ instead of from the combinational structure. We replaced the gradient descent method with Newton's method to speed up Ricci flow completion by tens of times. We named this novel algorithm the *discrete variational Ricci flow*. A practical system for computing hyperbolic and real projective structures for real surfaces has been developed based on discrete variational Ricci flow.

Circle packing was first introduced by Thurston in the seventies in [3]. A practical software system for circle packing with improved algorithm can be found in [12], which considers the combinatorial structure of the triangulation only. Recently, circle packing has been generalized to circle patterns [24,20] and used for surface parameterization in [10], which focuses on Euclidean geometry. Circle packing, circle pattern and discrete Ricci flow can be unified using the derivative cosine law [21].

Our work is based on a novel theoretical tool — discrete variational Ricci flow — and focuses on hyperbolic structure and real projective structure instead of Euclidean structure. Furthermore the hyperbolic metrics computed using our method are conformal to the original metrics. The conformal hyperbolic metrics convey much geometric information of the surfaces, which are valuable for the purposes of shape analysis.

3. Theoretical background

In this section we briefly introduce the major concepts from algebraic topology, differential geometry and Riemann surface to explain geometric structures on surfaces, and review discrete Ricci flow needed in the current work. We limit ourselves to those concepts that are directly relevant to our work. For detailed explanations, we refer readers to [4,8].

3.1. Uniformization theorem

Suppose Σ is an oriented surface in $\mathbb{R}^3$, with induced Euclidean metric g, and $u : \Sigma \to \mathbb{R}$ is a function defined on M, then $e^{2u}g$ is another metric for Σ, which is called *a metric conformal to g*.

The uniformization theorem claims that there exists a unique function u, such that under the metric $e^{2u}g$, the Gaussian curvatures of the interior points are constant, and the boundaries become geodesics. $e^{2u}g$ is called the *uniformization metric*. Surfaces with positive Euler numbers have spherical uniformization metrics with $+1$ curvature; surfaces with zero Euler number has flat uniformization metric with 0 curvature; surfaces with negative Euler numbers have hyperbolic uniformization metric with -1 curvature. The uniformization metrics will induce the spherical, Euclidean, and hyperbolic structures respectively, see Fig. 2.

3.2. Fundamental group and universal cover

Two curves are *homotopic* to each other, if they can deform to each other on the surface. Closed loops are classified to

homotopy classes by homotopic relation. Two closed curves sharing common points can be concatenated to form another loop. This operation defines the multiplication of homotopic classes. Therefore, all the base pointed homotopy classes form the so called *the first fundamental group* of Σ, and are denoted as $\pi_1(\Sigma)$.

The fundamental group is finitely generated. Suppose a surface Σ is with g handles, and there are two distinct generators a, b on each handle. If they intersect once, but disjoint with generators on other handles, then all g pairs of generators form a set of *canonical fundamental group basis*, denoted as $\{a_1, b_1, a_2, b_2, \ldots, a_g, b_g\}$.

Suppose that $\bar{\Sigma}$ and Σ are surfaces, then $(\bar{\Sigma}, \pi)$ is said to be a *covering space* of Σ if π is surjective and locally homeomorphic. Furthermore, if $\bar{\Sigma}$ is simply connected, $(\bar{\Sigma}, \pi)$ is the *universal covering space* of Σ.

A transformation of the universal covering space $\phi :\bar{\Sigma} \to \bar{\Sigma}$ is a *deck transformation*, if $\pi = \pi \circ \phi$. All deck transformations form a group G. It is also called the *Fuchsian group* of Σ if the transformation is hyperbolic isometry.

The deck transformation group is isomorphic to the fundamental group. Suppose $p \in \Sigma$ is an arbitrary point on Σ, its pre-images are $\pi^{-1}(p) = \{p_0, p_1, p_2, \ldots, p_n, \ldots\}$ on $\bar{\Sigma}$. Suppose a deck transformation $\phi \in G$ maps p_0 to p_k, then a curve on the universal covering space

$$\gamma : [0, 1] \to \bar{\Sigma}, \qquad \gamma(0) = p_0, \quad \gamma(1) = p_k,$$

connects p_0 and p_k and its projection $\pi(\gamma)$ is a loop on Σ. The homotopy class of $\pi(\gamma)$ is solely determined by p_0 and p_k, independent of the choice of γ. By this way, we get a bijective map from deck transformations to the first fundamental group of Σ.

A *fundamental domain F* is a subset of $\bar{\Sigma}$, such that the universal covering space is the union of conjugates of F, and any two conjugates have no interior point in common. Given a canonical fundamental group generators $\{a_1, b_1, a_2, b_2, \ldots, a_g, b_g\}$, we can slice Σ along the curves and get a fundamental domain with boundary $a_1 b_1 a_1^{-1} b_1^{-1} a_2 b_2 a_2^{-1} b_2^{-1} \cdots a_g b_g a_g^{-1} b_g^{-1}$.

For any surface Σ, its uniformization metric is also a metric for its universal cover $\bar{\Sigma}$. The universal cover can be isometrically embedded in one of the three canonical spaces: sphere, plane and hyperbolic space.

3.3. Hyperbolic space models

One of the anomalies of hyperbolic geometry was the realization that it has no isometric embedding in Euclidean space. Here are two common non-isometric embeddings for hyperbolic geometry: one is the Poincaré model, the other is the Klein model.

3.3.1. Poincaré model
The Poincaré model is a unit disk $\mathbb{D}^2$ in the complex plane with the Riemannian metric $ds^2 = \frac{4dz d\bar{z}}{(1-z\bar{z})^2}$.

The geodesics are circular arcs perpendicular to the boundary of the unit disk $\partial \mathbb{D}^2$. The isometric transformation

in this model is the so called Möbius transformation with the form

$$\phi(z) = e^{i\theta} \frac{z - z_0}{1 - \bar{z}_0 z}, \quad z, z_0 \in \mathbb{C}, \theta \in [0, 2\pi).$$

The above Möbius transformation maps z_0 to the center of the disk, and rotates the whole disk by angle θ. Hyperbolic circles are also Euclidean circles.

The Poincaré model is a conformal model, whereas the Klein model is a real projective model.

3.3.2. Klein model
The Klein model is another model of the hyperbolic space also defined on the unit disk $\mathbb{D}^2$. Any geodesic in the Klein model is a chord of the unit circle of the boundary of $\mathbb{D}^2$. The map from the Poincaré model to the Klein model is $\beta : \mathbb{H}^2 \to \mathbb{D}^2$,

$$\beta(z) = \frac{2z}{1 + \bar{z}z}, \qquad \beta^{-1}(z) = \frac{1 - \sqrt{1 - \bar{z}z}}{\bar{z}z} z. \tag{5}$$

Any Möbius transformation ϕ in the Poincaré model becomes a real projective transformation $\beta \circ \phi \circ \beta^{-1}$ in the Klein model.

3.4. Discrete surface Ricci flow

Ricci flow is a powerful tool to compute the uniformization metrics. It is a process to deform the metric $\mathbf{g}(t)$ according to its induced Gauss curvature $K(t)$, where t is the time parameter

$$\frac{dg_{ij}(t)}{dt} = -K(t)g_{ij}(t). \tag{6}$$

The following theorem postulates that Ricci flow defined in (6) converges, and the metric $\mathbf{g}(t)$ is conformal to the original one at any time t. Eventually, the Gauss curvature will become a constant. The corresponding metric $\mathbf{g}(\infty)$ is the desired uniformization metric.

Theorem 1 (*Hamilton 1982*). *For a closed surface of non-positive Euler characteristic, if the total area of the surface is preserved during the flow, the Ricci flow will converge to a metric such that the Gaussian curvature is constant everywhere.*

The spherical case is shown in the following theorem,

Theorem 2 (*Chow*). *For a closed surface of positive Euler characteristic, if the total area of the surface is preserved during the flow, the Ricci flow will converge to a metric such that the Gaussian curvature is constant every where.*

Recently, Ricci flow on 3-manifolds has been applied for the proof of Poincaré conjecture [30–32].

But in engineering fields, smooth surfaces are often approximated by discrete surfaces with triangulations. In the following, we discuss the discrete Ricci flow theory, which considers triangular mesh Σ with vertex set V, edge set E and face set F.

Discrete Riemannian metric. The Riemannian metric on an Euclidean or hyperbolic mesh S (we say a mesh is Euclidean or hyperbolic if all its faces are Euclidean or hyperbolic) is

determined by its edge lengths. Therefore we define the discrete Riemannian metric on a mesh as its edge lengths, $l : E \to \mathbb{R}^+$, such that for a face $\{i, j, k\}$, the edge lengths satisfy the triangle inequality, $l_{ij} + l_{jk} > l_{ki}$. Because the above triangle inequality is linear, it is easy to verify that all the discrete Riemannian metrics for a given mesh form a convex polytope in $\mathbb{R}^n$, where n is the number of edges.

A *weight* on the mesh is a function $\Phi : E \to [0, \frac{\pi}{2}]$, on each edge e_{ij}. A *radius* on the mesh is a function $\Gamma : V \to \mathbb{R}^+$, on each vertex v_i by assigning a positive number γ_i. They realize each edge e_{ij} joining v_i to v_j by a Euclidean segment of length

$$l_{ij} = \sqrt{\gamma_i^2 + \gamma_j^2 + 2\gamma_i \gamma_j \cos \Phi(e_{ij})}. \tag{7}$$

And for each face, $\{l_{ij}, l_{jk}, l_{ki}\}$ satisfy triangle inequality. In the hyperbolic case, the length can be deduced from the hyperbolic cosine law:

$$l_{ij} = \cosh^{-1}(\cosh \gamma_i \cosh \gamma_j + \sinh \gamma_i \sinh \gamma_j \cos \Phi(e_{ij})). \tag{8}$$

Definition 3 (*Circle Packing Metric*). The pair of the vertex radius function and edge weight function on a mesh $\Sigma\{\Gamma, \Phi\}$ is called a *circle packing metric* of Σ.

Intuitively, circle packing metric can be interpreted in the following way: we associate each vertex v_i with a cone of radius γ_i. For each edge e_{ij}, two cones on v_i and v_j intersect each other with an angle Φ_{ij}. In the smooth case, a conformal deformation will map an infinitesimal circle to an infinitesimal circle with intersection angles preserved. Therefore, we can define two circle packing metrics on the same mesh which are conformally equivalent to each other.

Definition 4 (*Conformal Circle Packing Metrics*). Two circle packing metrics $\{\Gamma_1, \Phi_1\}$ and $\{\Gamma_2, \Phi_2\}$ are *conformally equivalent*, if $\Phi_1 \equiv \Phi_2$.

Therefore, a conformal deformation of a circle packing metric only modifies the vertex radii.

Discrete Gauss curvature. Discrete Gauss curvature is defined as the angle deficit on a mesh. For an interior vertex v_i, the discrete Gauss curvature is

$$K_i = 2\pi - \sum_{f_{ijk} \in F} \alpha_i^{jk}, \tag{9}$$

where α_i^{jk} represents the corner angle attached to vertex v_i in the face f_{ijk}. Similarly, for a boundary vertex, the discrete Gauss curvature is

$$K_i = \pi - \sum_{f_{ijk} \in F} \alpha_i^{jk}. \tag{10}$$

Continuous Ricci flow is the conformal deformation of the Riemannian metric, such that the deformation is proportional to the Gaussian curvature. Similarly, we can define discrete Ricci flow in the following

Definition 5 (*Discrete Ricci Flow*). On a Euclidean triangle mesh with circle packing metric, the Euclidean Ricci flow is

$$\frac{\mathrm{d}\gamma_i(t)}{\mathrm{d}t} = -K_i \gamma_i(t). \tag{11}$$

On a hyperbolic triangle mesh with circle packing metric, the discrete hyperbolic Ricci flow is

$$\frac{\mathrm{d}\gamma_i(t)}{\mathrm{d}t} = -K_i \sinh \gamma_i(t). \tag{12}$$

The following theoretical results guarantee the convergence of the discrete Ricci flow.

Theorem 6 (*Discrete Ricci Flow*). *The discrete Ricci flows* (11) *and* (12) *are convergent to the uniformization metric and the convergence rate is exponential.*

More theoretical details can be found in [8].

Discrete Ricci flows can be treated as the gradient flows of minimizing special energies.

Definition 7 (*Discrete Ricci Energy*). Let $u_i = \ln \gamma_i$ in Euclidean case, $u_i = \ln \tanh \frac{\gamma_i}{2}$ in hyperbolic case, then the Euclidean Ricci energy and hyperbolic Ricci energy are defined as

$$f(\mathbf{u}) = \int_{\mathbf{u}_0}^{\mathbf{u}} \sum_{i=1}^{n} K_i \mathrm{d}u_i, \tag{13}$$

where $\mathbf{u} = (u_1, u_2, \dots, u_n)$, $\mathbf{u}_0 = (0, 0, \dots, 0)$.

The energy is defined on the space formed by all conformal circle packing metrics, which is simply connected. The integration path from $\mathbf{u}_0$ to $\mathbf{u}$ can be arbitrarily chosen, while the energy is consistent. The Hessian matrix for both the Euclidean Ricci energy and hyperbolic Ricci energy are positive definite, therefore their energies are convex, existing as a unique global minimal point. Instead of using discrete Ricci flow (11) and (12), we can directly minimize the Ricci energy using Newton's method, which is much more efficient in practice.

4. Algorithms to compute geometric structures on surfaces

For any surface with boundaries, we can convert it to a closed symmetric surface using the double covering method [16]. First we make two copies of the surface, then we reverse the orientation of one of them and glue the two copies along their corresponding boundaries. The double covered surface admits a uniformization metric conformal to its original metric and the original boundary curves become geodesics under this metric. The real projective structures of the original surface and its double covering can be induced by this uniformization metric. Therefore, in the following discussion, we only focus on closed surfaces.

4.1. Genus zero surface

Closed genus zero surfaces have spherical structures and real projective structures. The universal covering space of a closed genus zero surface is itself. Therefore, the surface can be conformally mapped to the unit sphere.

A method based on nonlinear heat flow to construct conformal maps between a closed genus zero surface and the unit sphere $\mathbb{S}^2$ is introduced in [18]. The spherical uniformization metrics are induced by these conformal maps.

The real projective structure can be deduced from the spherical structure directly. We set six tangent planes at the intersection points between the unit sphere and the axes, then project the sphere onto these tangent planes using central projection. This procedure produces the real projective atlas for the surface. Fig. 4 demonstrates the spherical structure and real projective structure of a closed genus zero surface.

4.2. Genus one surface

Closed genus one surfaces have affine structures which can be treated as special cases of real projective structures, and can be induced from surfaces' flat uniformization metrics where Gaussian curvatures are zero everywhere. The universal covering space of a closed genus one surface can be embedded in the Euclidean plane. Each fundamental domain is a parallelogram, and the deck transformations are translations on the plane. There are two methods to compute the flat uniformization metrics for closed genus one surfaces.

4.2.1. Holomorphic 1-form method

The flat uniformization metric on a closed genus one surface can be induced by the holomorphic 1-forms on it. A holomorphic 1-form can be treated as a pair of vector fields with zero divergence and curl, and orthogonal to each other. The algorithms for computing holomorphic 1-forms are introduced in [16,17]. By integrating one of its holomorphic 1-forms, the universal covering space of a closed genus one surface can be conformally mapped to the plane, which induces an affine atlas for the surface.

4.2.2. Discrete Euclidean Ricci flow method

The flat uniformization metric on a closed genus one surface can also be computed using the *discrete Euclidean Ricci flow method*. This method is particularly good for surfaces with boundaries compared with the holomorphic 1-form method which has to produce singularities on genus one surfaces with boundaries.

Given a triangular mesh, we first compute a circle packing metric $\{\Gamma, \Phi\}$ (see Eq. (7)) to approximate its induced Euclidean metric. Then we use Newton's method to minimize the Euclidean Ricci energy, see Eq. (13). The Hessian matrix of the energy is

$$\frac{\partial^2 f}{\partial u_i \partial u_j} = \frac{\partial K_i}{\partial u_j} = \frac{\partial K_i}{\partial r_j} r_j.$$

The Hessian matrix is positive definite, therefore the energy is strictly convex, with a unique global minimum. Newton's method can be used to find the minimum with stable convergence.

4.3. High genus surface

High genus surfaces have hyperbolic structures and real projective structures. Both of them can be induced from hyperbolic uniformization metrics on surfaces. The following algorithms are designed to compute the hyperbolic uniformization metric, hyperbolic structure and real projective structure for a given surface Σ with genus g greater than one.

(1) Compute a canonical homology basis and canonical fundamental domain of the surface Σ.
(2) Compute hyperbolic uniformization metric of the surface Σ using discrete hyperbolic Ricci flow method.
(3) Compute its Fuchsian group generators in the Poincaré disk model.
(4) Construct a hyperbolic atlas.
(5) Convert the hyperbolic atlas to the real projective atlas.

The algorithm in the first step, computing canonical homology basis and canonical fundamental domain, has been studied in computational topology and computer graphics literature [23,22]. We adopted the methods introduced in [6]. The following discussion will explain other steps in detail.

4.3.1. Compute hyperbolic uniformization metric

The *discrete hyperbolic Ricci flow* method is simple and powerful for computing the uniformization metrics of high genus surfaces. Comparing with Euclidean Ricci flow, there are two major differences

(1) Suppose a triangular face on the mesh with edge lengths, instead of treating it as a triangle in the Euclidean space, we treat it as a triangle in hyperbolic space. Then all the angles in the triangle can be calculated using the hyperbolic cosine law (8).
(2) In the energy form in Eq. (13), let $u_i = \ln \tanh \frac{\gamma_i}{2}$, therefore the Hessian matrix of the energy f is

$$\frac{\partial^2 f}{\partial u_i \partial u_j} = \frac{\partial K_i}{\partial r_j} \sinh r_j.$$

The other parts of the algorithm are identical to those of the Euclidean Ricci flow. The hyperbolic Ricci energy is strictly convex, with a unique global minimum, which gives us the desired hyperbolic uniformization metric.

4.3.2. Compute Fuchsian group generators in the Poincaré disk model

This step aims to compute the canonical Fuchsian group generators used for computing the universal covering space and hyperbolic structure in the next step.

4.3.2.1. Compute fundamental group generators. We first compute a set of canonical fundamental group generators $\{a_1, b_1, a_2, b_2, \ldots, a_g, b_g\}$. Assume the base point is p, then a_i's and b_j's are closed loops through the base point. The surface S is sliced open along the fundamental group generators to form a topological disk F called the canonical fundamental domain. The boundary of F has the form $\partial F = a_1 b_1 a_1^{-1} b_1^{-1} a_2 b_2 a_2^{-1} b_2^{-1} \cdots a_g b_g a_g^{-1} b_g^{-1}$.

4.3.2.2. Isometric embed in hyperbolic disk. We isometrically embed the universal covering space $\bar{\Sigma}$ onto the Poincaré disk using the uniformization metric computed from Section 4.3.1, and let $\phi : \bar{\Sigma} \to \mathbb{H}^2$ denote the isometric embedding.

We first select a face f_{012} from Σ arbitrarily. Suppose three edge lengths are $\{l_{01}, l_{12}, l_{20}\}$, and the corner angles are $\{\theta_0^{12}, \theta_1^{20}, \theta_2^{01}\}$ under the uniform hyperbolic metric. We simply embed the triangle as

$$\phi(v_0) = 0, \qquad \phi(v_1) = \frac{e^{l_{01}} - 1}{e^{l_{01}} + 1}, \qquad \phi(v_2) = \frac{e^{l_{02}} - 1}{e^{l_{02}} + 1} e^{i\theta_0^{12}}.$$

Then we can embed all the faces which share an edge with the first embedded face. Suppose a face f_{ijk} is adjacent to the first face, and vertices v_i, v_j have been embedded. A hyperbolic circle is denoted as $(\mathbf{c}, r)$, where $\mathbf{c}$ is the center, and r is the radius. Then $\phi(v_k)$ should be one of the two intersection points of the two hyperbolic circles $(\phi(v_i), l_{ik})$ and $(\phi(v_j), l_{jk})$. Also, the orientation of $\phi(v_i), \phi(v_j), \phi(v_k)$ should be counterclockwise. In the Poincaré model, a hyperbolic circle $(\mathbf{c}, r)$ coincides with an Euclidean circle $(\mathbf{C}, R)$, satisfying

$$\mathbf{C} = \frac{2 - 2\mu^2}{1 - \mu^2 |\mathbf{c}|^2} \mathbf{c}, \qquad R^2 = |\mathbf{C}|^2 - \frac{|\mathbf{c}|^2 - \mu^2}{1 - \mu^2 |\mathbf{c}|^2},$$

where $\mu = \frac{e^r - 1}{e^r + 1}$. So the intersection points between two hyperbolic circles can be found by intersecting the two corresponding Euclidean circles. The orientation of triangles can also be determined using Euclidean geometry on the Poincaré disk.

We can continuously embed faces which share edges with embedded faces in the same manner, until we embed enough portion of the whole $\bar{\Sigma}$ onto the Poincaré disk.

4.3.2.3. Compute Fuchsian group generators. Given two pairs of points (p_0, q_0) and (p_1, q_1) in the Poincaré disk, such that the geodesic distance from p_0 to q_0 equals that from p_1 to q_1. Then there exists a unique Möbius transformation ϕ, such that $p_1 = \phi(p_0)$ and $q_1 = \phi(q_0)$. ϕ can be constructed in the following way: construct a Möbius transformation ϕ_0 mapping p_0 to the origin and q_0 to a positive real number, with

$$\phi_0 = e^{-i\theta_0} \frac{z - p_0}{1 - \bar{p}_0 z}, \qquad \theta_0 = \arg \frac{q_0 - p_0}{1 - \bar{p}_0 q_0}.$$

Similarly, we can define another Möbius transformation ϕ_1, which maps p_1 to the origin, q_1 to a real number, and $\phi_1(q_1)$ equal to $\phi_0(q_0)$. Then the desired Möbius transformation ϕ is: $\phi = \phi_1^{-1} \circ \phi_0$.

Let $a_k, a_k^{-1} \subset \partial F$ are two boundary curve segments with their starting and ending vertices $\partial a_k = q_0 - p_0$ and $\partial a_k^{-1} =$

$p_1 - q_1$, then the Mobius transformation $(p_0, q_0) \to (p_1, q_1)$ is the Fuchsian generator β_k corresponding to b_k. In fact, β_k maps a_k to a_k^{-1}. Similarly, we can compute α_k which maps b_k^{-1} to b_k. Therefore, we can compute a set of canonical Fuchsian group generators $\{\alpha_1, \beta_1, \alpha_2, \beta_2, \ldots, \alpha_g, \beta_g\}$ corresponding to the set of canonical fundamental group generators $\{a_1, b_1, a_2, b_2, \ldots, a_g, b_g\}$ computed from Section 4.3.2.1.

4.3.3. Construct hyperbolic structure

With the computed universal covering space and the Fuchsian group generators, now we can construct the hyperbolic structure of the given surface now. First we construct a family of open sets $\{U_\alpha\}$, such that the union of the open sets covers the surface Σ, $\Sigma \subset \bigcup U_\alpha$. Then we locate a pre-image of each U_α in the universal covering space $\bar{\Sigma}$, as $\pi^{-1}(U_\alpha)$. The embedding of the pre-image $\pi^{-1}(U_\alpha)$ in the Poincaré disk gives the local coordinates of U_α, namely

$$\phi_\alpha := \phi \circ \pi^{-1}$$

where ϕ is the embedding map for the universal covering space to the Poincaré disk. If one point $p \in \Sigma$ on the surface Σ is covered by two charts (U_α, ϕ_α) and (U_β, ϕ_β), suppose $p_\alpha \in \bar{U}_\alpha$ and $p_\beta \in \bar{U}_\beta$, and a curve connecting p_α, p_β is denoted as γ. The homotopy class of $\pi(\gamma)$ is determined by p_α, p_β, denoted as $[\bar{p}_\alpha, \bar{p}_\beta]$. Assume $[\bar{p}_\alpha, \bar{p}_\beta] = \gamma_1 \gamma_2 \gamma_3 \cdots \gamma_n$, where γ_k is one of the a_i's or b_i's, we replace a_i in $[\bar{p}_\alpha, \bar{p}_\beta]$ by α_i, b_i by β_i in γ to get the chart transition map $\phi_{\alpha\beta}$ with the form

$$\phi_{\alpha\beta} = \phi_1 \circ \phi_2 \circ \phi_3 \cdots \phi_n,$$

where ϕ_j is one of the α_i's or β_i's. Therefore we construct a hyperbolic atlas $\{(U_\alpha, \phi_\alpha)\}$ which induces the hyperbolic structure of the surface.

4.3.4. Construct real projective structure

For a closed surface Σ with genus $g > 1$, its real projective atlas can be deduced from its hyperbolic structure (but the reverse is not true). Suppose $\{(U_\alpha, \phi_\alpha)\}$ is a hyperbolic atlas of Σ, then a real projective atlas $\{(U_\alpha, \tau_\alpha)\}$ can be straightforwardly constructed. Let

$$\tau_\alpha = \beta \circ \phi_\alpha \quad \text{and} \quad \tau_{\alpha\beta} = \beta \circ \phi_{\alpha\beta} \circ \beta^{-1},$$

where β is the map from the Poincaré model to the Klein model defined in Eq. (5).

Suppose ϕ_α has the form

$$\phi_\alpha = e^{i\theta} \frac{z - z_0}{1 - \bar{z}_0 z},$$

where $z_0 = x_0 + iy_0$, we use homogeneous coordinates (xw, yw, w) to parameterize the points (x, y) on the Klein model, then the transition map $\tau_{\alpha\beta}$ has the following form: $\tau_{\alpha\beta} = \frac{1}{\lambda} OT$, where $\lambda = x_0^2 + y_0^2 - 1$, and O is the rotation matrix. O and T are:

$$O = \begin{pmatrix} \cos\theta & -\sin\theta & 0 \\ \sin\theta & \cos\theta & 0 \\ 0 & 0 & 1 \end{pmatrix},$$
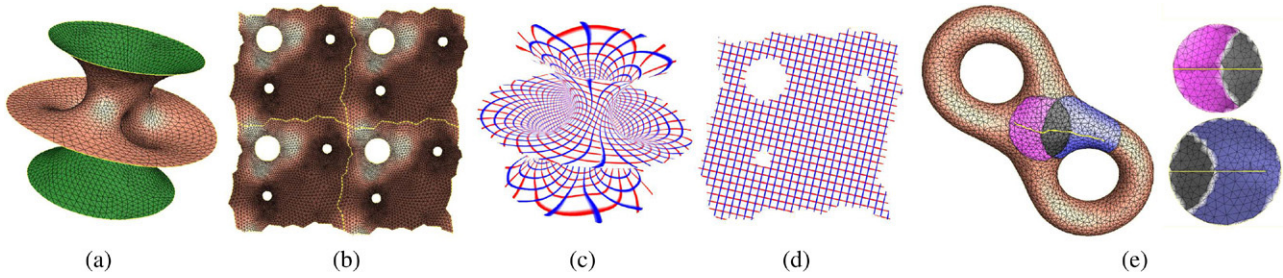
Fig. 3. Visualization of affine and real projective invariants: (a) Genus one hyper-sheet surface with three boundaries. (b) Its affine structure: a finite portion of its universal covering space embedded on the plane. (c) Parallel lines w.r.t. to the affine structure on the hyper-sheet surface. (d) Parallel lines on one chart of the affine structure. (e) Two overlapping real projective charts of the eight model. In the overlapping part, a straight line on one chart is still a straight line on the other chart.

Fig. 4. Genus zero David head model: (a) David head model. (b) Spherical structure. (c) Projective structure: six charts.
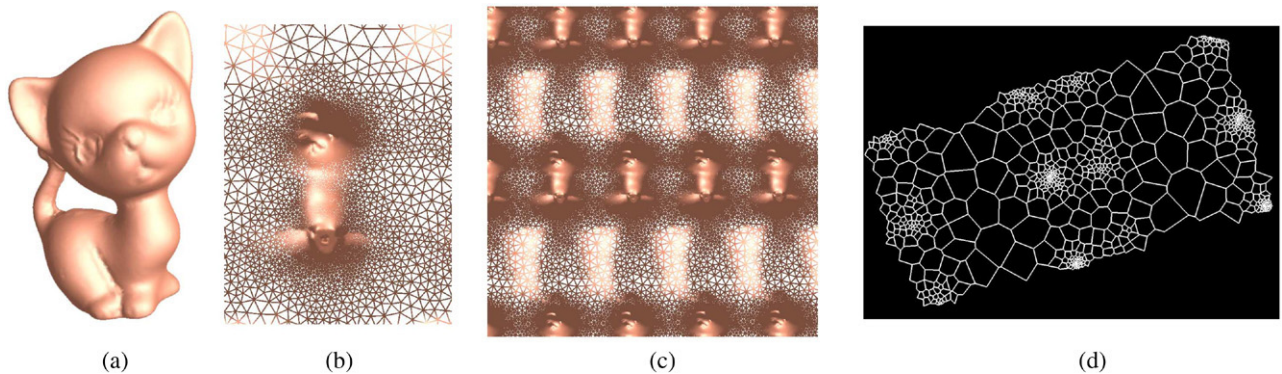
Fig. 5. Genus one kitten model: (a) Kitten model. (b) One chart on the plane. (c) Its Euclidean (affine) structure: a finite portion of its universal covering space on the plane. (d) The Voronoi diagram algorithm generalized on the surface via its Euclidean structure, four fundamental domains are shown.

$$T = \begin{pmatrix} 1 + x_0^2 - y_0^2 & 2x_0 y_0 & -2x_0 \\ 2x_0 y_0 & 1 - x_0^2 + y_0^2 & -2y_0 \\ 2x_0 & 2y_0 & -1 - x_0^2 - y_0^2 \end{pmatrix} \neq 0. \quad (14)$$

5. Applications

We apply geometric structures for various applications, which demonstrate the generality and the simplicity of this methodology. The experimental results also show the feasibility and the practical value of discrete variational Ricci flow.

5.1. Visualize geometric structures on surfaces

Although geometric structures are natural structures on surfaces, due to their abstract and intricate nature, they are difficult to perceive and understand. Furthermore, because of the lack of a feasible way to compute them, geometric structures are still not broadly appreciated and applied. In this paper, we visualize common geometric structures on

general surfaces by using modern graphics and visualization techniques. Fig. 3(a)–(d) shows the fact that parallelism can be defined on surfaces coherently via their affine structures. While (e) illustrates a projective invariant, collinearity can be defined on a surface via projective structure. Fig. 4 shows the closed genus zero David head model with its spherical structure and the induced projective structure. Fig. 5(a)–(c) illustrates the closed genus one kitten model with its affine structure. Fig. 6 shows the hyperbolic structures of two genus zero surfaces with three boundaries. Figs. 7–11 visualize hyperbolic structures and real projective structures for surfaces with genus greater than one.

5.2. Generalize Voronoi diagram algorithm to surfaces

Closed genus one surfaces equip Euclidean uniformization metrics, which can induce flat embeddings of the original surfaces onto the plane, such that the planar Voronoi diagram algorithm can be directly generalized to surfaces. Fig. 5(d)
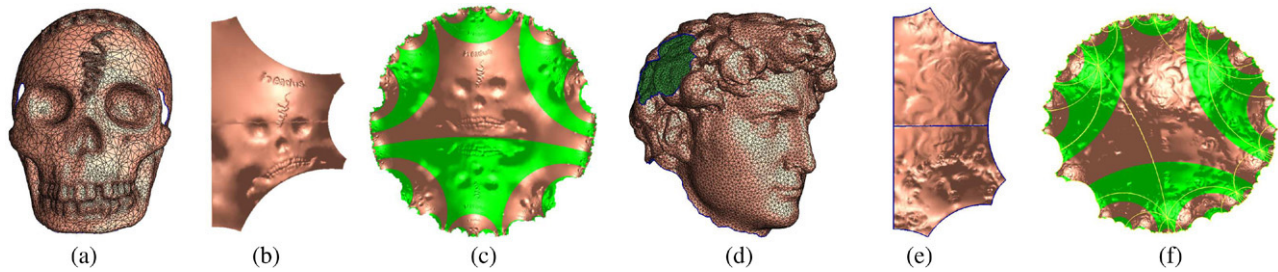
Fig. 6. Hyperbolic structure of genus zero surfaces with three boundaries: (a) Skull model. (b) One fundamental domain embedded in the Poincaré disk. (c) Its universal covering space embedded in the Poincaré disk. (d) David head model. (e) One fundamental domain embedded in the Poincaré disk. (f) Its universal covering space embedded in the Poincaré disk.
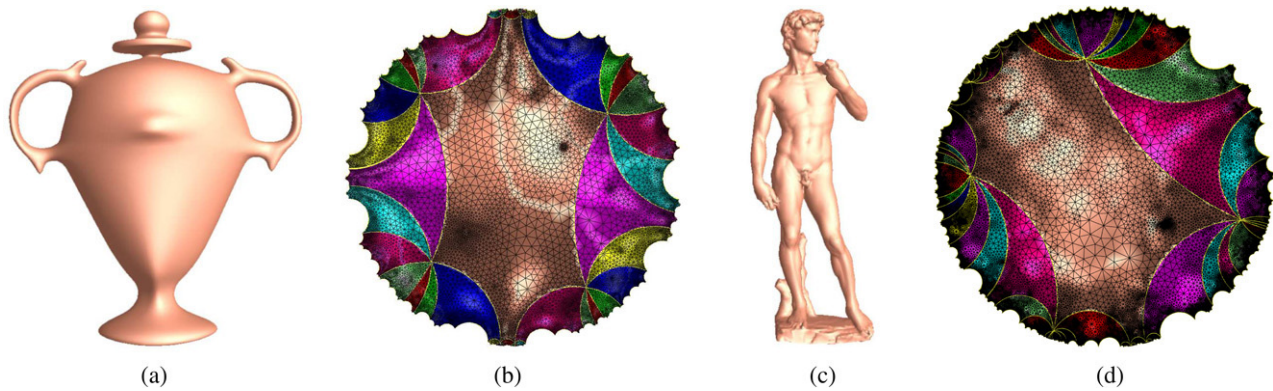
Fig. 7. Hyperbolic structure of World Cup model and David model. (a) Genus two World Cup model. (b) Hyperbolic structure induced from isometric embedding of Universal covering space in Poincaré model. (c) Genus three David model. (d) Hyperbolic structure induced from isometric embedding of Universal covering space in Poincaré model.
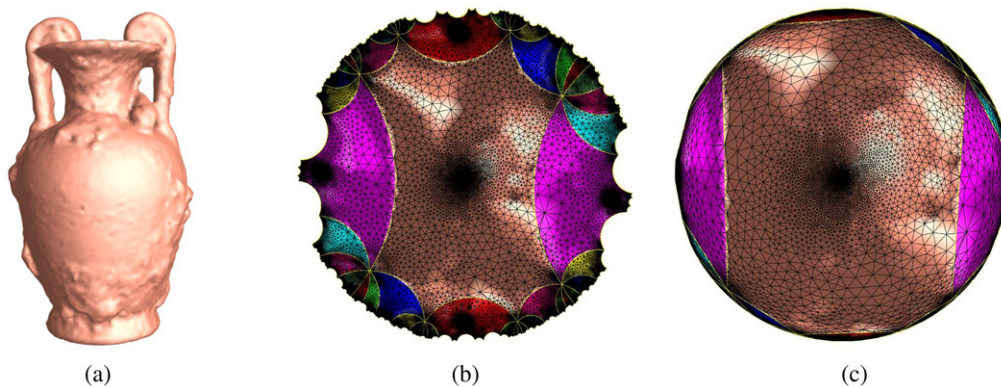
Fig. 8. Hyperbolic structure and real projective structure of amphora model. (a) Genus two amphora model. (b) Hyperbolic structure induced from isometric embedding of Universal covering space in the Poincaré model. (c) Real projective structure induced from isometric embedding of Universal covering space in the Klein model.

shows the Voronoi diagram algorithm generalized to the kitten model via its Euclidean structure, where the Voronoi diagram is depicted on a finite portion of the universal covering space.

5.3. Cross parameterizations

The cross parameterization between two different surfaces with identical topology has many useful applications, including surface metamorphosis, texture transfer, registration, shape comparison and so on [27]. However, when the given two surfaces have complicated topologies, it is very challenging to get the cross parameterization between them [28,27].

Using the uniformization metrics and Ricci flow, the cross parameterization between two different surfaces (Σ_1, Σ_2) can be easily carried out. First, we compute their canonical fundamental domains (F_1, F_2); then we compute their uniformization metrics and embed the fundamental domains onto the corresponding canonical space; finally, we construct a harmonic map which maps the embedded fundamental domains to each other. The harmonic map induces a map between two surfaces. Fig. 12 shows the cross parameterization between the two high genus surfaces. The left most and right most are the two surfaces' conformal embedding onto the Poincaré disk derived from the discrete hyperbolic Ricci flow.
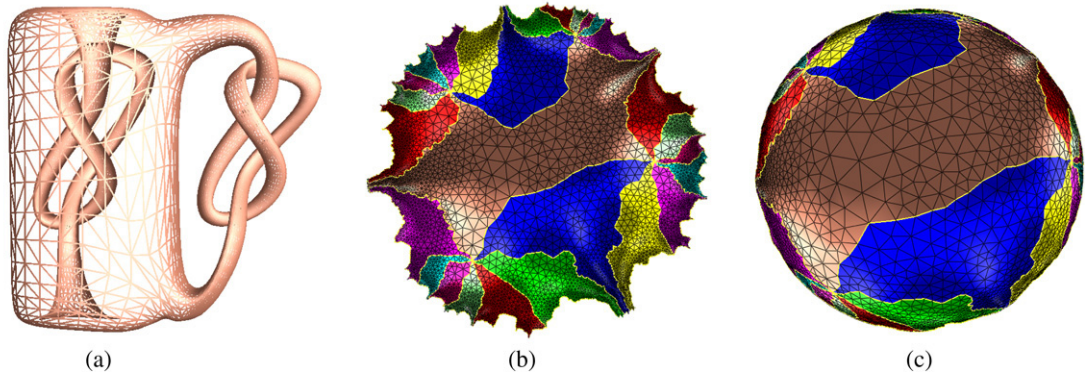
Fig. 9. Hyperbolic structure and real projective structure of knotty model. (a) Genus two knotty model. (b) Hyperbolic structure induced from isometric embedding of Universal covering space in the Poincaré model. (c) Real projective structure induced from isometric embedding of Universal covering space in the Klein model.
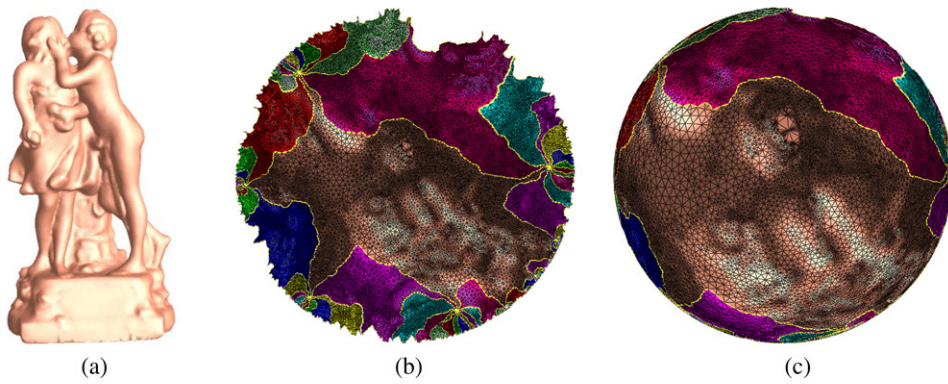
Fig. 10. Hyperbolic structure and real projective structure of sculpture model. (a) Genus three Sculpture model. (b) Hyperbolic structure induced from isometric embedding of Universal covering space in the Poincaré model. (c) Real projective structure induced from isometric embedding of Universal covering space in the Klein model.
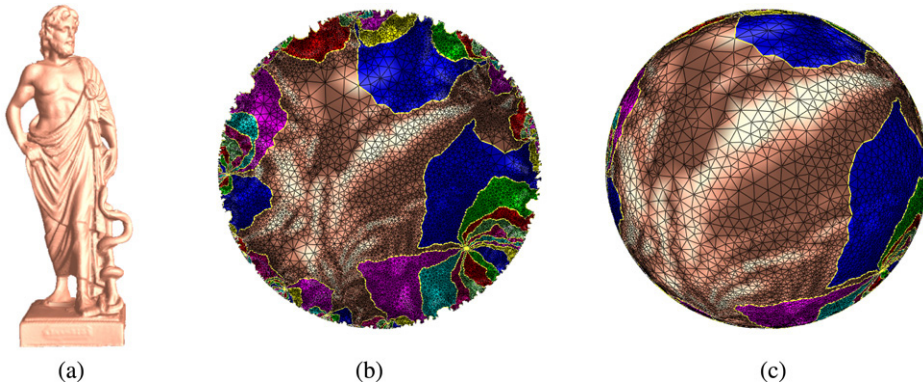
Fig. 11. Hyperbolic structure and real projective structure of Greek Sculpture model. (a) Genus four Greek Sculpture model. (b) Hyperbolic structure induced from isometric embedding of Universal covering space in the Poincaré model. (c) Real projective structure induced from isometric embedding of Universal covering space in the Klein model.

Fig. 12. Cross parameterization between two genus two surfaces.
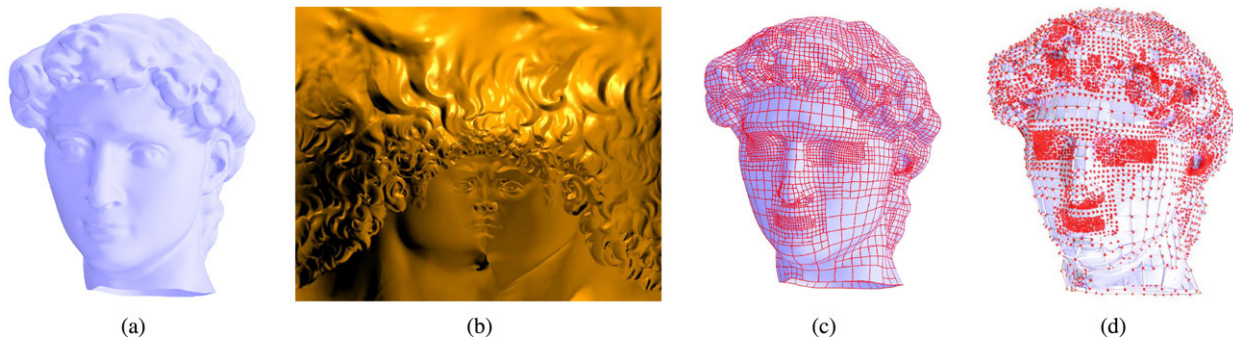
Fig. 13. Manifold T-spline: constructing T-spline surface from an affine atlas computed using Euclidean Ricci flow. (a) David head model. (b) Flat metric induces affine structure. (c) Manifold T-spline surface with knots structure. (d) Control net.
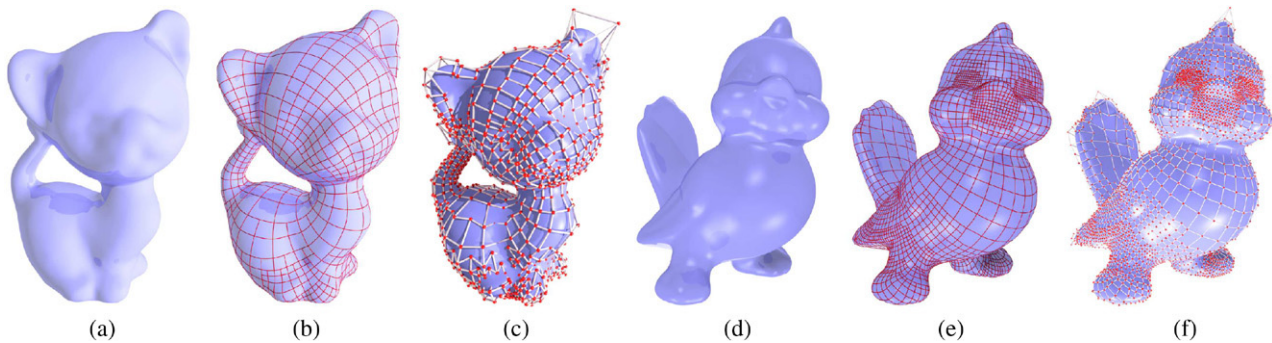
Fig. 14. More examples of manifold T-spline: (a) Kitten model. (b) Manifold T-spline kitten. (c) Control net. (d) Bird model. (e) Manifold T-spline bird. (f) Control net.
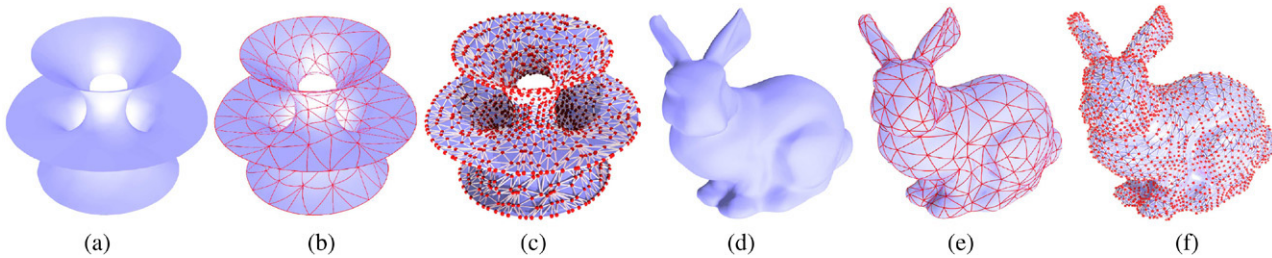
Fig. 15. Manifold Triangle B-spline: (a) Hyper-sheet model. (b) Manifold Triangle B-spline hyper-sheet. (c) Control net. (d) Bunny model. (e) Manifold Triangle B-spline bunny (f) Control net.

5.4. Manifold splines

Conventional splines are defined on planar domains. However, it is natural to define splines directly on surfaces with general topologies. The concept of manifold splines was first introduced in [19], where the splines are defined on manifold domains and the evaluations of the splines are independent of the choice of the local charts. The significant advantage of the manifold splines is that it is defined globally, and locally on each chart, it is similar to a conventional planar spline.

It has been proved that defining splines over arbitrary manifolds is equivalent to the existence of an affine atlas of the underlying manifold, so the key to construct a manifold spline is to construct the affine structure on the surface. The affine structures derived from Ricci flow are applied for constructing manifold T-splines and triangular B-splines shown in Figs. 13–15.

6. Conclusion

This work proposes a novel theoretic framework, geometric structures on general surfaces, which has fundamental importance in geometric modeling fields. Geometric structures allow different geometries to be defined on surfaces, therefore planar algorithms can be systematically generalized to manifold domains.

In order to compute geometric structures on arbitrary surfaces, we design and implement a powerful geometric tool, discrete variational Ricci flow, which can manipulate the Riemannian metrics on surfaces. So far, Ricci flow is the only way to compute hyperbolic and real projective structures.

Theoretically rigorous and practically efficient algorithms for computing affine structure, hyperbolic structure and real projective structure are thoroughly explained.

Extensive experiments are performed, which verify the solidness and feasibility of the algorithms. Geometric structures and Ricci flow are applied for several important applications, such as cross parameterizations, manifold splines etc.

Several important problems remain open. The real projective structure computed in this work is derived from hyperbolic structure. In theory, there exist real projective structures which are intrinsically different from the hyperbolic structure. We will explore alternative algorithm to compute them.

Conventional polar form splines are based on affine structure, which doesn't exist for general surfaces. Instead, projective structure exists for all surfaces. In order to define manifold splines based on projective structure, novel spline scheme based on projective invariants should be invented. We will investigate along this direction in the future.

References

[1] Milnor JW. On the existence of a connection with curvature zero. Comment Math Helv 1958;7(2):229–33.

[2] Benzècri JP. Variètès localement affines. Sem. topologie et gèm. diff., vol. 7. Ch. Ehresmann; 1959. p. 215–23.

[3] Thurston WP. Geometry and topology of 3-manifolds. Princeton Lecture notes. 1976.

[4] Thurston WP. Three-dimensional geometry and topology. Princeton University Presss; 1997.

[5] Grimm C, Hughes JF. Parameterizing *N*-holed tori. In: IMA conference on the mathematics of surfaces. 2003. p. 14– 29.

[6] Carner C, Jin M, Gu X, Qin H. Topology-driven surface mappings with robust feature alignment. IEEE Visualization 2005;543–50.

[7] Wallner J, Pottmann H. Spline orbifolds. Curves and surfaces with applications in CAGD. 1997. p. 445–64.

[8] Chow B, Luo F. Combinatorial Ricci flows on surfaces. Journal Differential Geometry 2003;63(1):97–129.

[9] Ferguson H, Rockwood AP, Cox J. Topological design of sculptured surfaces. In: SIGGRAPH. 1992. p. 149–56.

[10] Kharevych L, Springborn B, Schroder P. Discrete conformal mappings via circle patterns. ACM Trans Graphics 2005.

[11] Hamilton RS. The Ricci flow on surfaces. Math General Relativity 1988; 71:237–62.

[12] Stephenson K. Introduction to circle packing. Cambridge University Press; 2005.

[13] Haker S, Angenent S, Tannenbaum A, Kikinis R, Sapiro G, Halle M. Conformal surface parameterization for texture mapping. IEEE Trans Vis Comput Graph 2000;6(2):181–9.

[14] Gotsman C, Gu X, Sheffer A. Fundamentals of spherical parameterization for 3D meshes. ACM Trans Graph 2003;22(3):358–63.

[15] Praun E, Hoppe H. Spherical parametrization and remeshing. ACM Trans Graph 2003;22(3):340–9.

[16] Gu X, Yau S-T. Global conformal parameterization. In: Symposium on geometry processing. 2003. p. 127–37.

[17] Jin M, Wang Y, Yau S-T, Gu X. Optimal global conformal surface parameterization. IEEE Visualization 2004;267–74.

[18] Gu X, Wang Y, Chan TF, Thompson PM, Yau S-T. Genus zero surface conformal mapping and its application to brain surface mapping. IEEE Trans Med Imaging 2004;23(8):949–58.

[19] Gu X, He Y, Qin H. Manifold splines. Graphical Models 2006;68(3): 237–54.

[20] Bobenko AI, Schroder P. Discrete Willmore flow. In: Eurographics symposium on geometry processing. 2005.

[21] Luo W, Gu X. Discrete curvature flow and derivative cosine law. 2006. Preprint.

[22] Erickson JG, Whittlesey K. Greedy optimal homotopy and homology generators. In: Proc. 16th symp. discrete algorithms. ACM and SIAM; 2005. p. 1038–46.

[23] de Verdière C, Éric, Lazarus F. Optimal system of loops on an orientable surface. In: Proceedings of the 43rd annual IEEE symposium on foundations of computer science. 2002. p. 627–36.

[24] Bobenko AI, Springborn BA. Variational principles for circle patterns and Koebe's theorem. Trans Amer Math Soc 2004;356:659.

[25] Jin M, Luo F, Gu X. Computing surface hyperbolic structure and real projective structure. In: ACM symposium on solid and physics modeling. 2006.

[26] Gunn C. Visualizing non-Euclidean geometry. In: Proceedings of Bolyai bicentennial conference. 2004. p. 121–41.

[27] Schreiner J, Asirvatham A, Praun E, Hoppe H. Inter-surface mapping. ACM Trans Graph 2004;23(3):870–7.

[28] Kraevoy V, Sheffer A. Cross-parameterization and compatible remeshing of 3D models. ACM Trans Graph 2004;23(3):861–9.

[29] Goldman R. Computer graphics in its fifth decade: Ferment at the foundations. In: 11th Pacific conference on computer graphics and applications. 2003. p. 4–21.

[30] Perelman G. The entropy formula for the Ricci flow and its geometric applications, arXiv:org; November 11, 2002.

[31] Perelman G. Ricci flow with surgery on three-manifolds, arXiv:org; March 10, 2003.

[32] Perelman G. Finite extinction time for the solutions to the Ricci flow on certain three-manifolds, arXiv:org; July 17, 2003.